



Lab resource: Stem Cell Line

Generation of the human induced pluripotent stem cell (hiPSC) line PSMi005-A from a patient carrying the KCNQ1-R190W mutation

Manuela Mura^a, Yee-Ki Lee^{b,c,d}, Federica Pisano^{a,e}, Monia Ginevrino^{f,g}, Marina Boni^h, Federica Calabrò^a, Lia Crotti^{i,j,k}, Enza Maria Valente^{f,g}, Peter J. Schwartzⁱ, Hung-Fat Tse^{b,c,d}, Massimiliano Gneccchi^{a,e,l,*}

^a Coronary Care Unit, Laboratory of Experimental Cardiology for Cell and Molecular Therapy, Fondazione IRCCS Policlinico San Matteo, Pavia, Italy

^b Cardiology Division, Department of Medicine, the University of Hong Kong, Hong Kong SAR, China

^c Hong Kong-Guangdong Joint Laboratory on Stem Cell and Regenerative Medicine, the University of Hong Kong, Hong Kong SAR, China

^d Guangzhou Institutes of Biomedicine and Health, China

^e Department of Molecular Medicine, Unit of Cardiology, Università degli studi di Pavia, Pavia, Italy

^f Department of Molecular Medicine, Unit of Genetics, Università degli studi di Pavia, Pavia, Italy

^g Neurogenetics Unit, Fondazione IRCCS Santa Lucia, Rome, Italy

^h Laboratory of Oncohaematological Cytogenetic and Molecular Diagnostics, Division of Haematology, Fondazione IRCCS Policlinico San Matteo, Pavia, Italy

ⁱ Center for Cardiac Arrhythmias of Genetic Origin and Laboratory of Cardiovascular Genetics, Istituto Auxologico italiano, IRCCS, Milan, Italy

^j Department of Cardiovascular, Neural and Metabolic Sciences, San Luca Hospital, Istituto Auxologico italiano, IRCCS, Milan, Italy

^k Department of Medicine and Surgery, Università Milano-Bicocca, Milan, Italy

^l Department of Medicine, University of Cape Town, Cape Town, South Africa

ABSTRACT

We generated human induced pluripotent stem cells (hiPSCs) from dermal fibroblasts of a woman carrier of the heterozygous mutation c.568C > T p.R190W on the *KCNQ1* gene. hiPSCs, obtained using four retroviruses encoding the reprogramming factors OCT4, SOX2, cMYC and KLF4, display pluripotent stem cell characteristics, and can be differentiated into spontaneously beating cardiomyocytes (hiPSC-CMs).

Resource table

Unique stem cell line identifier	PSMi005-A	Gene/locus	568C > T mutation on <i>KCNQ1</i> , 11p15.5-p15.4 (NM_000218.2)
Alternative name of stem cell line	HDF29-LQT1-iPS	Method of modification	N/A
Institution	Fondazione IRCCS Policlinico San Matteo, Pavia, Italy	Name of transgene or resistance	N/A
Contact information of distributor	Massimiliano Gneccchi, m.gneccchi@unipv.it	Inducible/Constitutive system	N/A
Type of cell line	hiPSC	Date archived/stock date	Jan 7, 2013
Origin	human	Cell line repository/bank	No
Additional origin info	Age: 37 Gender: female Ethnicity: Caucasian	Ethical approval	The study has been approved by the Ethics Committee of our Institution, Fondazione IRCCS Policlinico San Matteo, on the 29th of October 2010, protocol number 20100004354, proceeding P-20100003369. We obtained patient written informed consent for both skin biopsy procedure and conservation of biological samples.
Cell source	Dermal fibroblasts		
Clonality	Clonal		
Method of reprogramming	Retroviruses encoding for the human cDNA of OCT4, SOX2, cMYC, KLF4		
Genetic modification	No		
Type of modification	N/A		
Associated disease	Long QT Syndrome type 1 (OMIM #192500)		

Resource utility

It has been proven that iPSCs and iPSC-CMs can be efficiently used to model LQTS and test targeted therapies (Mehta et al., 2018; Gneccchi

* Corresponding author at: IRCCS Policlinico S. Matteo, Università di Pavia and Fondazione, Pavia, Italy.

E-mail address: m.gneccchi@unipv.it (M. Gneccchi).

<https://doi.org/10.1016/j.scr.2019.101437>

Received 4 March 2019; Received in revised form 21 March 2019; Accepted 11 April 2019

Available online 13 April 2019

1873-5061/ © 2019 The Authors. Published by Elsevier B.V. This is an open access article under the CC BY-NC-ND license (<http://creativecommons.org/licenses/by-nc-nd/4.0/>).

et al., 2017; Mura et al., 2017; Rocchetti et al., 2017). PSMi005-A cell line will be of help to: (1) modelling of LQTS type 1; (2) targeted drug testing.

Resource details

The PSMi005-A cell line was generated by reprogramming of dermal fibroblasts derived from a skin biopsy of 37 years old woman diagnosed with Long QT Syndrome type 1 (LQT1). LQTS is an autosomal dominant inherited disease characterized by the prolongation of cardiac repolarization, reflected by a prolongation of the QT interval on the surface electrocardiogram (ECG) (Schwartz et al., 2012). The repolarization defect predisposes to “Torsades de Pointes” (TdP), a type of ventricular tachycardia that can cause syncope or even sudden cardiac death (SCD). LQT1 is the most common LQTS sub-type, accounting for ~40–50% of all LQTS cases. It is caused by mutations in the *KCNQ1* gene, encoding for the α -subunit of the voltage-dependent potassium channel responsible for the delayed rectifier potassium current (I_{Ks}), one of the repolarization currents in the heart (Schwartz et al., 2012).

The patient carries the heterozygous mutation c.568C/T on the *KCNQ1* gene, that causes the substitution of the arginine in position 190 with tryptophan. Despite the fact that her QTc (QT corrected for heart rate) in basal condition is normal and she never experienced cardiac symptoms, she was placed in preventive therapy with propranolol 2.0 mg/kg/die.

Fibroblasts were reprogrammed by retroviral infection of OCT4, SOX2, KLF4 and c-MYC. The hiPSCs were maintained on feeders. The disease causing mutation on the *KCNQ1* gene is present on both patient's fibroblasts and the derived hiPSCs, as shown by DNA sequencing (Fig. 1A. *The KCNQ1 coding sequence -CDS- used as a reference is the NCBI sequence NM_000218.2*). They also present an identical DNA profile at 7 polymorphic loci, as shown by Short tandem Repeat (STR) analysis (available with authors). Moreover the DNA karyotyping revealed normal female features (46, XX) (Fig. 1B). PSMi005-A retains embryonic stem cell (ES)-like morphology and pluripotent features up to passage 50 (Fig. 1C). It uniformly expresses the human ES surface antigens Tumor Related Antigen-1-60 and – 1-81 (TRA-1-60, TRA-1-81), Stage Specific Embryonic Antigen-4 (SSEA-4), and shows alkaline phosphatase (AP) activity (Fig. 1C). Likewise, it expresses the pluripotent markers NANOG, OCT4, SOX2, REX1, GDF3, ESG1, DPPA2, DPPA4 and NODAL (Fig. 1C and D), and shows OCT4 promoter demethylation (Fig. 1E, *open circles indicate unmethylated CpG dinucleotides, while closed circles indicate methylated CpGs*). The percentage of NANOG⁺ cells determined by immunocytochemistry counting was 99.4%, (Fig. 1F). RT-PCR analysis in Fig. 1G shows no expression of the four viral transgenes (Tg) in naïve fibroblasts (HDF), clear expression of Tg OCT4, SOX2, KLF4 and cMYC in fibroblasts 5 days after transduction (OSKM) and silencing of the four Tg in PSMi005-A at passage 3.

As expected, PSMi005-A spontaneously forms embryoid bodies (EBs) able to differentiate into cells belonging to the three germ layers: endoderm (alpha-fetoprotein-AFP), mesoderm (alpha smooth muscle actin- α SMA, troponin I- TnI) and ectoderm (tubulin beta III-Tuj, microtubule-associated protein 2-MAP2) (Fig. 1H). Moreover, PSMi005-A differentiated also into spontaneously beating cardiomyocytes, expressing the sarcomeric proteins alpha-actinin (α -SA) and troponin T (TnT) (Fig. 1I, *the insets show areas of cross-striation*). We also verified the absence of mycoplasma contamination in our PSMi005-A line (Fig. 1J).

Materials and methods

Detailed protocols are provided as Supplemental Methods.

hiPSC generation

Skin fibroblasts were reprogrammed using four retroviruses encoding OCT4, SOX2, KLF4 and c-MYC. Emerging iPSC clones were manually picked, individually placed into a separate cell culture well and expanded on a feeder-layer of mitotically-inactivated mouse embryonic fibroblasts (iMEF), in DMEM/F12, 20% Knockout Serum Replacement (KO-SR), 2 mM L-glutamine, 50 U/ml penicillin, 50 U/ml streptomycin, 1% Non-Essential Amino Acids (NEAA), 0.1 mM beta-mercaptoethanol, 10 ng/ml basic Fibroblast Growth Factor (bFGF) (Table 1).

Mutation analysis

KCNQ1 exon 3 was amplified with primers in Table 2 and the GoTaq G2 DNA polymerase (Promega). The resulting amplicon (size in Table 2) was purified and sequenced (Lightrun service - GATC Biotech AG – Germany).

STR analysis

STR analysis was carried out using PowerPlex® CS7 System (Promega) kit, following the manufacturer's protocol. Fragments were run on a 3130xl capillary sequencer (Applied Biosystems). Genotypes were assigned using GeneMarker software (SoftGenetics).

Karyotyping

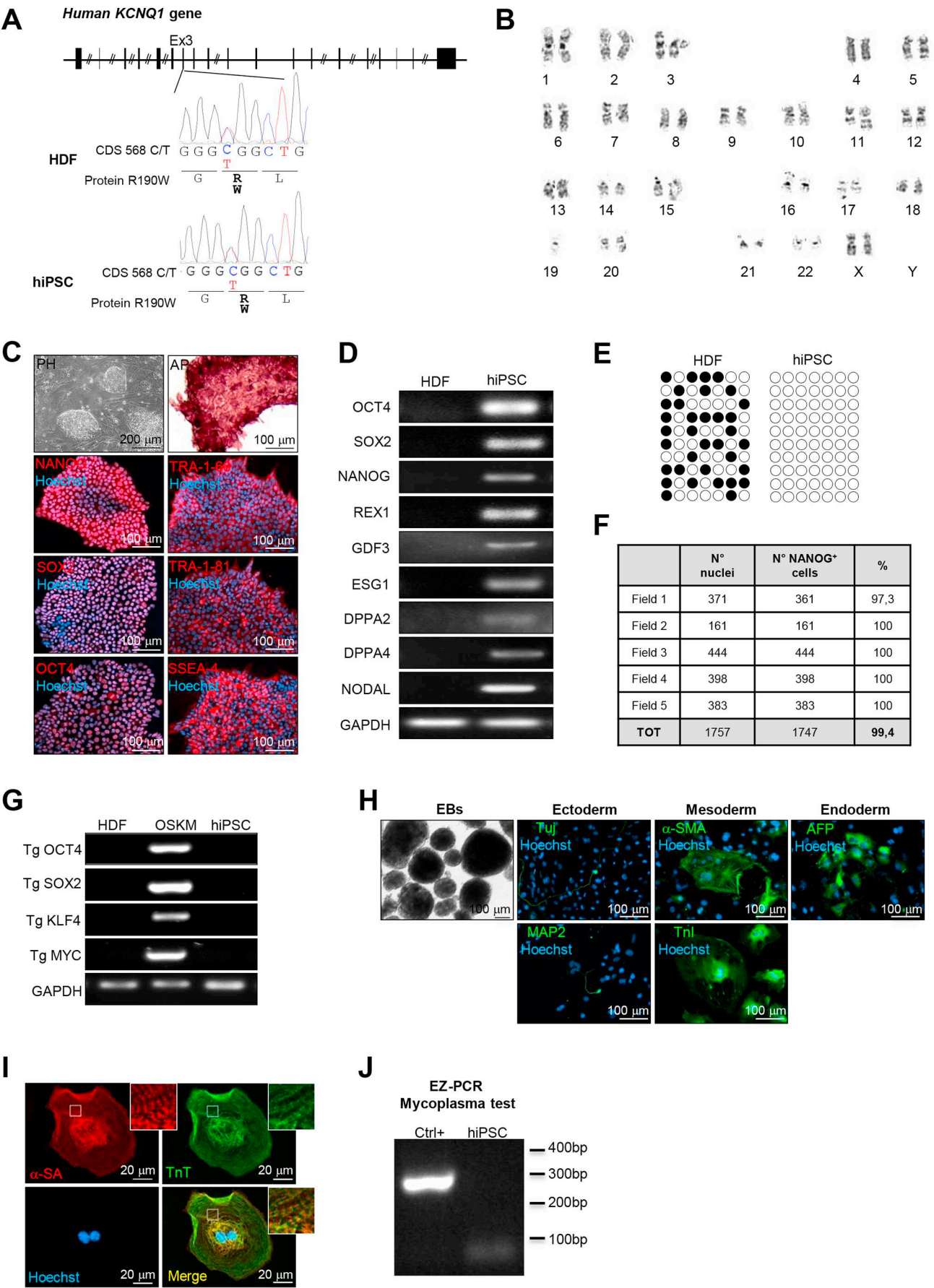
hiPSCs were blocked at metaphase by exposition to 10 μ g/ml demecolcine solution (Sigma Aldrich) for 3 h. Karyotyping was performed using 300 G-banding chromosome analysis.

Immunocytochemistry

hiPSCs and their derivatives were grown on glass coverslips, and then fixed for 15 min in 4% paraformaldehyde (Affymetrix USB), permeabilized with 0.1% Triton X-100 (Sigma Aldrich) for 5 min, and blocked in 1% bovine serum albumin (BSA, Sigma Aldrich) for 1 h at room temperature (RT). Then they were incubated for 1 h at RT with the primary antibody (Table 2) diluted in blocking solution, washed three times, and incubated for 1 h at RT with an appropriate secondary antibody (Table 2). Finally, the cells were stained with 1 μ g/ml of Hoechst 33258 (Sigma Aldrich). Images were acquired using the Carl Zeiss fluorescence microscope Observer.Z1 equipped with the Apotome system and AxioVision 6.0 software (Zeiss GmbH, Gottingen, Germany).

Immunocytochemistry counting

Nanog⁺ cells and the nuclei stained with Hoechst 33258 were counted in five fields using the AxioVision 6.0 software (Zeiss GmbH, Gottingen, Germany).



(caption on next page)

Fig. 1. Characterization of the PSMi005-A cell line. **A.** Top: schematic representation of *KCNQ1* gene (exons are vertical lines/boxes). The *KCNQ1* coding sequence (CDS) used as a reference is the NCBI sequence NM_000218.2. Bottom: DNA sequencing results showing the mutation 568 C/T in the *KCNQ1* gene in heterozygosis in both patient-derived dermal fibroblasts (HDF) and PSMi005-A cell line (hiPSC). **B.** Karyotype analysis of PSMi005-A (300 G-bands) showing normal female karyotype (46, XX). **C.** Top left: phase contrast image showing PSMi005-A morphology (PH). Top right: alkaline phosphatase colorimetric staining (AP). Bottom panels: immunofluorescence stainings showing uniform expression of pluripotency markers in the PSMi005-A. Nuclei were counterstained with Hoechst 33258 (Hoechst, blue). **D.** RT-PCR analysis showing expression of the indicated markers of pluripotency in PSMi005-A (hiPSC) compared with its parental fibroblasts (HDF). **E.** *OCT4* promoter methylation analysis with bisulfite sequencing in patient's dermal fibroblasts (HDF) and in the derived hiPSCs. Open circles indicate unmethylated CpG dinucleotides, while closed circles indicate methylated CpGs. **F.** Immunocytochemistry counting of anti Nanog-positive (Nanog⁺) cells. The total number of cells in each of the five fields analyzed was quantified by counting the nuclei stained with Hoechst 33258. **G.** RT-PCR analysis showing no expression of the four viral transgenes (Tg) in naïve fibroblasts (HDF), expression of Tg *OCT4*, *SOX2*, *KLF4* and *cMYC* five days after transduction (OSKM) and silencing of the four Tg in PSMi005-A at passage 6. **H.** Far left panel: floating embryoid bodies (EBs) formed after 7 days of PSMi005-A culture in suspension. Panels on the right: immunofluorescence staining for markers of the 3 germ layers in iPSC-derived EBs: neuronal class tubulin beta III (Tuj) and microtubule-associated protein 2 (MAP2) for ectoderm, smooth muscle actin (α -SMA) and troponin I (TnI) for mesoderm, and alpha Fetoprotein (AFP) for endoderm. **I.** Co-immunofluorescence staining for the alpha-sarcomeric actinin (α -SA, red) and troponin T (TnT, green) in cardiomyocytes differentiated from the PSMi005-A. Nuclei were counterstained with Hoechst 33258 (Hoechst, blue). Magnifications show areas of cross-striations. **J.** EZ-PCR test showing the absence of mycoplasma contamination in PSMi005-A. Ctrl + is the positive PCR control provided by the kit.

Table 1
Characterization and validation of PSMi005-A cell line.

Classification	Test	Result	Data
Morphology	Photography	Normal	Fig. 1 panel C
Phenotype	Qualitative analysis	Positive immunostaining for the pluripotency markers <i>OCT4</i> , <i>NANOG</i> , <i>SOX2</i> , <i>TRA-1-60</i> , <i>TRA-1-81</i> , <i>SSEA-4</i>	Fig. 1 panel C
		Positive staining for the alkaline phosphatase	Fig. 1 panel C
		Expression of the pluripotency markers <i>OCT3/4</i> , <i>SOX2</i> , <i>NANOG</i> , <i>Rex1</i> , <i>GDF3</i> , <i>ESG1</i> , <i>DPPA2</i> , <i>DPPA4</i> , <i>NODAL</i> measured by RT-PCR	Fig. 1 panel D
	Quantitative analysis	99,4% <i>NANOG</i> ⁺ cells quantified by immunocytochemistry counting	Fig. 1 panel F
Genotype	Karyotype (300 G-banding) and resolution	46XX, Resolution 450–500	Fig. 1 panel B
Identit	Microsatellite PCR (mPCR)	Not performed	Not available
	STR analysis	7 sites tested for iPSC, all sites matched with donor HDF STR profile	Available with authors
Mutation analysi	Sequencing	Heterozygous for the mutation c. 568C > T p.R190W on the <i>KCNQ1</i> gene	Fig. 1 panel A
Microbiology and virology	Mycoplasma	Mycoplasma testing by RT-PCR. Negative	Fig. 1 panel J
Differentiation potential	Embryoid body formation	The EBs expressed neuronal class tubulin beta III (Tuj) and microtubule-associated protein (MAP) (ectoderm); smooth muscle actin (SMA) and troponin I (mesoderm); alpha Fetoprotein (AFP) (endoderm).	Fig. 1 panel H
	Differentiation into cardiomyocytes	The iPSC-derived cardiomyocytes expressed the cardiac sarcomeric proteins alpha-sarcomeric actinin (α -SA) and troponin T (TnT)	Fig. 1 panel I
Donor screening	HIV 1 + 2 Hepatitis B, Hepatitis C	Not performed	Not available
Genotype additional info	Blood group genotyping	Not performed	Not available
	HLA tissue typing	Not performed	Not available

AP assay

AP was detected by using the Alkaline Phosphatase Staining kit (00–0009 Stemgent).

RT-PCR

Total RNA was purified using TRIzol (ThermoFisher). cDNA was synthesized using the Superscript II Reverse Transcriptase (ThermoFisher). RT-PCR was performed with the GoTaq G2 DNA polymerase (Promega) and primers in Table 2.

OCT4 promoter demethylation analysis

Genomic DNA were treated with the EZ DNA methylation kit (Zymo Research, Orange, CA, USA). The promoter region of the human *OCT4* gene was amplified with biotinylated primers (Table 2) using Amplitaq

gold 360 (Applied Biosystems). PCR products were sequenced (sequencing primer sequence in Table 2) using Pyrosequencing PSQ96 HS System (Biotage, Uppsala, Sweden). The methylation status of each locus was analyzed using PyroQ-CpG software (Qiagen).

EB formation

hiPSCs were grown for 7 days in suspension in a modified iPSC medium deprived of bFGF and containing 20% FBS instead of KO-SR. Forming EBs were then transferred to gelatin-coated dishes to allow differentiation in adhesion for additional 7 days, and finally immunostained for the three germ layers.

Cardiac differentiation

Cardiac differentiation was induced using the PSC Cardiomyocyte Differentiation Kit (ThermoFisher).

Table 2
Reagents details.

Antibodies used for immunocytochemistry			
	Antibody	Dilution	Company Cat # and RRID
<i>Pluripotency Markers</i>	Rabbit anti NANOG	1:200	Stemgent Cat# 09-0020, RRID: AB_2298294
	Mouse anti OCT3/4 (C-10)	1:500	SCBT Cat# sc-5279, RRID: AB_628051
	Mouse anti SOX2	1:500	R&D Systems Cat# MAB2018, RRID: AB_358009
	Mouse anti TRA-1-60	1:100	Stemgent Cat# 09-0010, RRID: AB_1512170
	Mouse anti TRA-1-81	1:100	Stemgent Cat# 09-0011, RRID: AB_1512171
	Mouse anti SSEA-4	1:100	Stemgent Cat# 09-0006, RRID: AB_1512169
<i>Differentiation Markers (EBs)</i>	Mouse anti neuronal class tubulin beta III (Tuj)	1:500	Covance Cat# MMS-435P, RRID: AB_2313773
	Anti microtubule-associated protein 2 (MAP2)	1:200	Millipore Cat# MAB3418, RRID: AB_94856
	Mouse anti smooth muscle actin	1:1000	Millipore Cat# CBL171, RRID: AB_2223166
	Mouse anti Troponin I (TnI)	1:200	Millipore Cat# MAB1691, RRID: AB_2256304
<i>Cardiac Markers</i>	Mouse anti alpha-fetoprotein	1:500	Millipore Cat# SCR030, RRID: AB_597591
	Mouse anti Troponin T ^a	1:250	ThermoFisher Cat# MA5-12960, RRID: AB_11000742
	Mouse anti alpha actinin ^a	1:800	Sigma Aldrich Cat# A7811, RRID: AB_476766
<i>Secondary antibodies</i>	Alexa-Fluor® 546 Goat anti-rabbit IgG	1:500	ThermoFisher Cat# A11010, RRID: AB_143156
	Alexa-Fluor® 488 Goat anti-mouse IgG	1:500	ThermoFisher Cat# A11001, RRID: AB_2534069
	Alexa-Fluor® 546 Goat anti-mouse IgG	1:500	ThermoFisher Cat# A11003, RRID: AB_141370
Primers			
	Target	Forward/Reverse primer (5'-3')	
<i>Targeted mutation analysis/sequencing</i>	<i>KCNQ1</i> Exon 3	Fw: 5'-gttcaaacagggttcagggtctga -3'	Rev.: 5'-ccaggtttccagaccaggaag -3'
	256 bp	Fw: 5'-gtactctcgtgctcccttttc-3'	Rev.: 5'-caaaaacccctggcacaact-3'
<i>Pluripotency Markers (RT-PCR)</i>	OCT4	Fw: 5'-acaccaatcccatccacact-3'	Rev.: 5'-tctctgctgaggtgaggtat-3'
	168 bp	Fw: 5'-ttcttctcctcatggatctg-3'	Rev.: 5'-tctgctgaggtgaggtat-3'
	SOX2	Fw: 5'-cagatcctaacaagctcgcagaat-3'	Rev.: 5'-cggtacgcaaatataagtcaga-3'
	273 bp	Fw: 5'-cttatgctacgtaaaggagctggg-3'	Rev.: 5'-gtgccaaccaggtcccggaagt-3'
	NANOG	Fw: 5'-atatcccgctgggtgaaagt-3'	Rev.: 5'-actcagccatggactggagcatcc-3'
	213 bp	Fw: 5'-ggagccgctgcccctggaat-3'	Rev.: 5'-ttttctctgatattctatccat-3'
	REX1	Fw: 5'-ccgtcccgcaatcctctccatc-3'	Rev.: 5'-atgatccaacatggctccgg-3'
	306 bp	Fw: 5'-gggcaaggacacgtcgacatca-3'	Rev.: 5'-gggactcgggtgggctgtaacgtttc-3'
	GDF3	Fw: 5'-catgtccaatatgattccacc-3'	Rev.: 5'-gggatctcgtctcggaagat-3'
	631 bp	Fw: 5'-ccccaggggccattttggtacc-3'	
	ESG1	Fw: 5'-ggcaccctggcatggtctcttggtc-3'	
	243 bp	Fw: 5'-caacaaccgaaatgcaccagccag-3'	
	DPPA4	Fw: 5'-acgatcgtggccccgaaaaggacc-3'	
	408 bp		
	DPPA2		
	606 bp		
	NODAL		
	234 bp		
<i>House-Keeping Genes (RT-PCR)</i>	GAPDH	Rev: 5'-cccttttctggagactaaataaa-3'	
	112 bp	Fw: 5'-gaggttgagtagaaggattgtttgttt-3'	Rev.: 5'-ccccctaaaccatcacctccaccaccta-3'
<i>Retroviral transgenes</i>	OCT4 cDNA on pMXs-hOCT3/4	Fw: 5'-agagagggttgagtagtttt-3'	
	339 bp		
	SOX2 cDNA on pMXs-hSOX-2		
	496 bp		
	cMYC cDNA on pMXs-hcMYC		
	542 bp		
<i>OCT4 promoter demethylation analysis/ Bisulfite sequencing</i>	KLF4 cDNA on pMXs-hKLF4		
	518 bp		
	pMX viral vector		
	OCT4 promoter		
	467 bp		
	Sequencing primer		

^a To perform the co-staining with these two antibodies, we used the Zenon Tricolor Mouse IgG labeling Kit (Molecular Probes)

Acknowledgements

This work was supported by the Leducq Foundation for Cardiovascular Research [18CVD05] ‘Towards Precision Medicine with Human iPSCs for Cardiac Channelopathies’, and by the Italian Ministry of Health, "Ricerca Corrente" projects numbers 08064017 and 08064018.

Appendix A. Supplementary data

Supplementary data to this article can be found online at <https://doi.org/10.1016/j.scr.2019.101437>.

References

Gnecchi, M., Stefanello, M., Mura, M., 2017. Induced pluripotent stem cell technology:

- toward the future of cardiac arrhythmias. *Int. J. Cardiol.* 237, 49–52.
- Mehta, A., Ramachandra, C.J.A., Singh, P., Chitre, A., Lua, C.H., Mura, M., Crotti, L., Wong, P., Schwartz, P.J., Gnecchi, M., Shim, W., 2018. Identification of a targeted and testable antiarrhythmic therapy for long-QT syndrome type 2 using a patient-specific cellular model. *Eur. Heart J.* 39, 1446–1455.
- Mura, M., Mehta, A., Ramachandra, C.J., Zappatore, R., Pisano, F., Ciuffreda, M.C., Barbaccia, V., Crotti, L., Schwartz, P.J., Shim, W., Gnecchi, M., 2017. The KCNH2-IVS9-28A/G mutation causes aberrant isoform expression and hERG trafficking defect in cardiomyocytes derived from patients affected by long QT syndrome type 2. *Int. J. Cardiol.* 240, 367–371.
- Rocchetti, M., Sala, L., Dreizehnter, L., Crotti, L., Sinnecker, D., Mura, M., Pane, L.S., Altomare, C., Torre, E., Mostacciolo, G., Severi, S., Porta, A., De Ferrari, G.M., George Jr., A.L., Schwartz, P.J., Gnecchi, M., Moretti, A., Zaza, A., 2017. Elucidating arrhythmogenic mechanisms of long-QT syndrome CALM1-F142L mutation in patient-specific induced pluripotent stem cell-derived cardiomyocytes. *Cardiovasc. Res.* 113, 531–541.
- Schwartz, P.J., Crotti, L., Insolia, R., 2012. Long-QT syndrome: from genetics to management. *Circ. Arrhythm. Electrophysiol.* 5, 868–877.